INTERNATIONAL JOURNAL OF ENERGY STUDIES

e-ISSN: 2717-7513 (ONLINE); homepage: https://dergipark.org.tr/en/pub/ijes

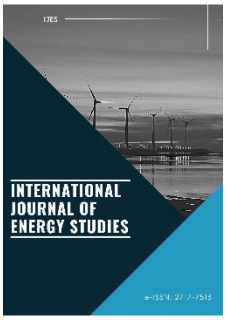

Research Article

Int J Energy Studies 2023; 8(3): 315-330

DOI: 10.58559/ijes.1291259

Received : 03 May 2023

Revised : 08 July 2023

Accepted : 27 July 2023

Performance analysis of dual-evaporator ejector refrigeration system in different configurations: Experimental investigation

Batuhan Üğüdür[a], Ümit İşkan[b], Mehmet Direk[c*]

[a]MAC Soğutma Sanayi ve Ticaret A.Ş. , 77600 Yalova, Turkey, ORCID:0000-0002-6969-2098

[b]Yalova University, Electricity and Energy Department, 77200 Yalova, Turkey,ORCID: 0000-0001-6236-2339

[c]Yalova University, Energy Systems Engineering Department, 77200 Yalova, Turkey, ORCID:0000-0001-5868-6381

*(*Corresponding Author: mehmet.direk@yalova.edu.tr)*

Highlights

- Assessed the effectiveness of an ejector in different configuration.
- Dual evaporator ejector refrigeration system was tested.
- It was determined that the ejector operates more efficiently in systems with dual evaporators

You can cite this article as: Ugudur B, Iskan U, Direk M. Performance analysis of dual-evaporator ejector refrigeration system in different configurations: Experimental investigation. Int J Energy Studies 2023; 8(3): 315-330.

ABSTRACT

This study aimed to assess the effectiveness of an ejector refrigeration cycle, using a laboratory-scale experimental system operating in different configurations. The investigated configurations consisted of a conventional vapour compression refrigeration (CVCR) system and a dual evaporator ejector system (DEES) operated in two modes: DEES with a single thermal expansion valve ($DEES_A$) and DEES with dual thermal expansion valves ($DEES_B$). The findings revealed that the utilization of the ejector enhanced the refrigerant's mass flow rate. Additionally, the $DEES_A$ configuration achieved higher cooling capacities compared to the CVCR. Moreover, the $DEES_A$ configuration achieved up to 21% higher coefficient of performance (COP) values. On the other hand, when the system was operated in the $DEES_B$ configuration, it yielded lower evaporation temperatures and higher superheating degrees in comparison to $DEES_A$. Based on the evaluations, it can be concluded that the ejector operates more efficiently in systems with dual evaporators, thereby making positive contributions to overall system performance.

Keywords: Ejector, TXV, COP, Dual evaporator

1. INTRODUCTION

Refrigeration systems account for approximately 20% of the total energy consumed in buildings, making it essential to use low energy-consuming refrigeration systems due to high energy prices [1]. The most widely used refrigeration cycles in buildings are conventional vapour compression refrigeration (CVCR) systems. To reduce the energy consumption of CVCR systems, modifications such as internal heat exchangers, expander-compressor and ejectors can be applied [2]–[5]. By using the ejector, throttling losses can be recovered and thus the energy consumption of the compressor can be diminished. In the literature, it was observed that the coefficient of performance (COP) of the refrigeration systems increases with the use of the ejector [6]. Ejector refrigeration cycles use a separator to separate the liquid and gas phases. However, separator is not 100% efficient, which can cause incomplete separation. To address this issue, some studies suggest using a second evaporator instead of a separator [7]–[9]. In their experimental study on ejector refrigeration systems, Bilir Sağ et al. [10] found that the highest COP was achieved with a 2.3 mm throat diameter ejector. Saban et al. [11] determined that the COP value increased by 21% compared to the conventional system when an ejector was used. Wang et al. [12] evaluated the performance of an ejector heat pump system. They observed COP increases ranging from 2.6% to 3.7%, depending on the refrigerant used. Geng et al. [13] conducted a study on the DEES to investigate the impact of the ejector on the system performance. They observed a COP improvement ranging from 16% to 30% compared to CVCR. In the study conducted by Carrillo et al. [14] the ejector refrigeration cycle was analyzed for different operating modes. R134a, R1234yf and R600a refrigerants were used in the study. It was determined that the efficiency of the system could increase up to 26% by using the ejector. Kim et al. [9] tested the DEES system at different entrainment ratios, compressor speeds, and ejector geometries. It was determined that the COP of DEES was 6.3% higher. In a theoretical comparison between DEES and a conventional refrigeration system, Gao et al. [15] determined that the exergy efficiency of DEES is 32.4% - 41.7% higher than the conventional system. Liu et al. [16] found that the COP of a DEES system was 15.9-27.1% higher than that of a CVCR system. In their study, Direk et al [17] found that the COP value obtained from the DEES system was 13.24% higher than that of the baseline system. In addition, the total exergy destruction in the DEES system was 28.8% lower compared to the conventional system [18]. Ünal et al. [19] conducted a study to assess the impact of employing different refrigerants on the dimensions of the ejector in the ejector-integrated bus air conditioning system. The study revealed that the size of the ejector is significantly influenced by the type of refrigerant used. The ejector technology can also be applied to heat pump systems. Direk et al.

[20] revealed that the COP for an ejector-integrated heat pump water heater was 5.5% higher compared to the baseline system, which did not utilize an ejector. Tahir Erdinç et al. [21] reported that the COP of an ejector heat pump system was 22.6% higher than the base system. Furthermore, Iskan and Direk [22] investigated the use of five different refrigerants (R1234ze(E), R515a, ND, R516A, R456A) in the DEES system in 2022 as an alternative to R134a. It was found that the highest performance values were obtained with R516A. Iskan et al. [23] tested the DEES system with R516A under varying water temperatures and flow rates. The was revealed that the mass flow rate of water passing through the evaporator#2 (the evaporator placed at the outlet of the ejector) had a greater impact on the system's performance than the ER. Further experimental studies are needed to better understand the performance and efficiency of ejector refrigeration systems operating in different configurations. In this study experiments were conducted using R134a refrigerant in different configurations of the system.

2. EXPERIMENTAL SYSTEM

The experimental system is designed to operate in various configurations. The system comprises the primary components of a traditional refrigeration system, including an ejector, water cycles, channels, tubes, valves, and bypass lines. Fig. 1 displays a picture of the experimental rig.

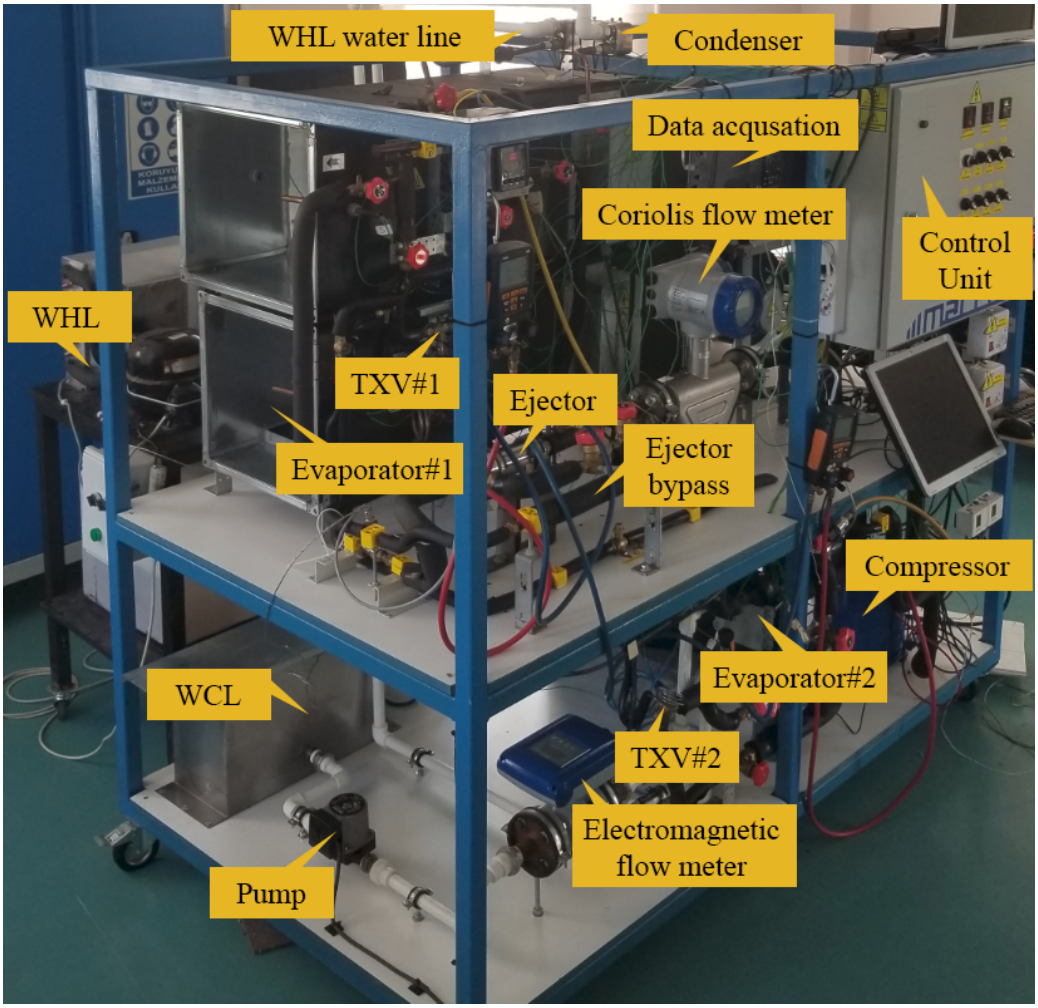

Figure 1. General view of the experimental system

In the experimental rig, there are two water loop connected with the heat exchangers. Among these, the water cooler loop (WCL) is connected to the evaporator#2 and the water heater loop (WHL) is connected to the condenser. At the beginning of the experiment, the water was brought to the desired temperatures with an electric heaters connected to the PID control unit in the water tanks. The refrigerant and water lines of the experimental rig are presented in Fig. 2.

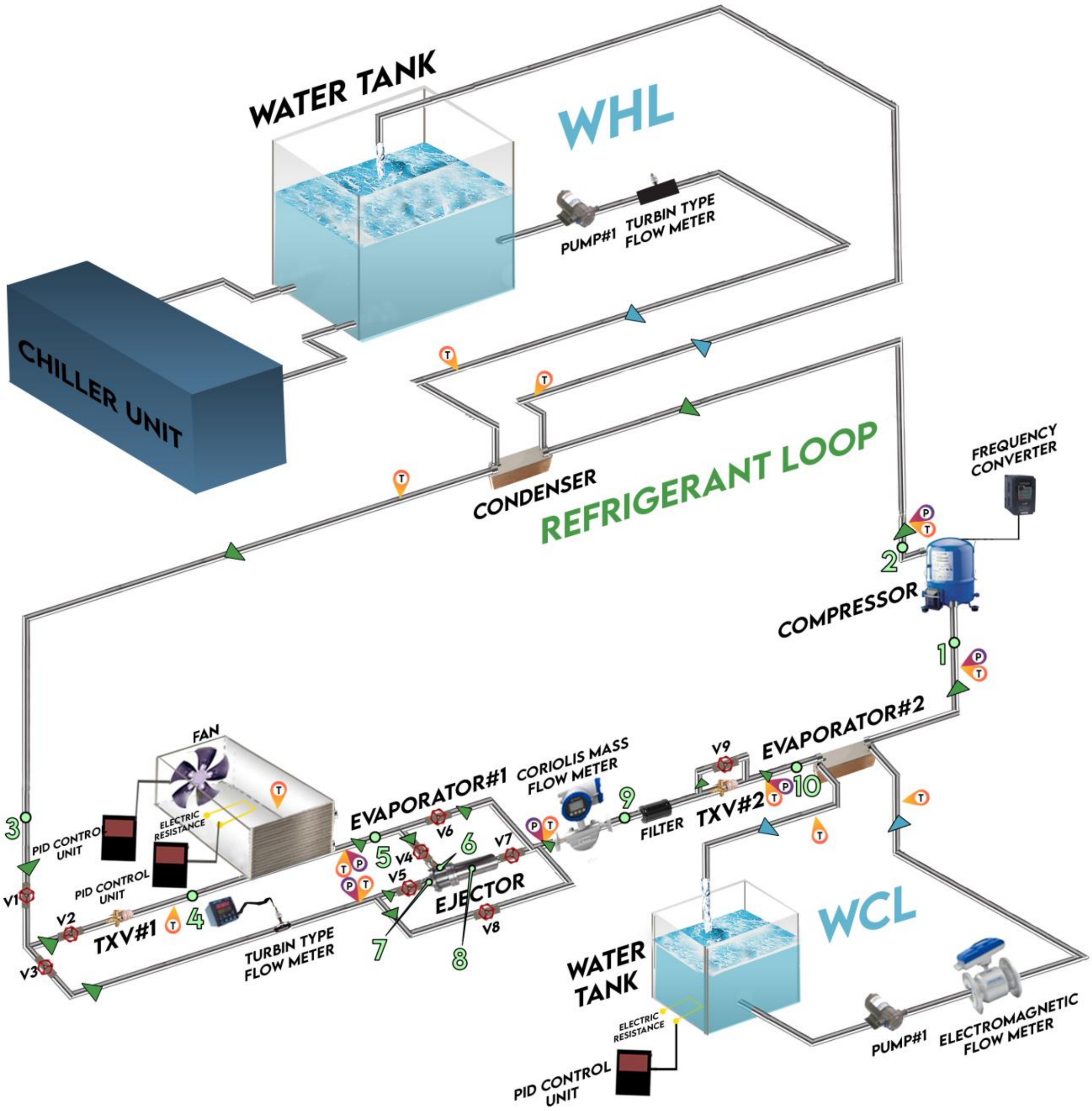

Figure 2. Schematic of experimental system

In the system, the condenser and evaporator#1 are positioned in a duct, and variable speed fans are placed at the entrance of these ducts to provide air flows at desired speeds. The air temperatures determined in the experiments are provided by using PID controlled electrical resistance heaters. In the experimental system, Danfoss MTZ022 brand hermetic (Vol: 30.23 cm^3/rev, 2900 RPM) compressor was used. The connections, switches and fuses of the PID systems are placed in a panel. Evaporator#2 water flow rate (accuracy ± 0.3 %) was measured with electromagnetic flow-meter. The mass flow rates of the refrigerant (accuracy ± 0.05 %) were measured with the Krohne brand Coriolis flowmeter. The mass flow meter is placed between the ejector outlet and the evaporator#2. The mass flow rate of the refrigerant flowing from the primary inlet of the ejector (condenser outlet) was measured with a turbine-type flow meter (accuracy of ±0.1%). In order to measure temperatures at various points in the system, a 40-channel temperature recording device was used. K-type thermocouples were utilized to measure the inlet and outlet temperatures of the refrigerant, air, and water flow and transferred to the recording device. Additionally, the refrigerant pressure at various points were measured using pressure transmitters and electronic manometers (with ±0.5% accuracy). The technical drawing of the injector used in the test system is given in Fig 3, its photograph is given in Fig 4.

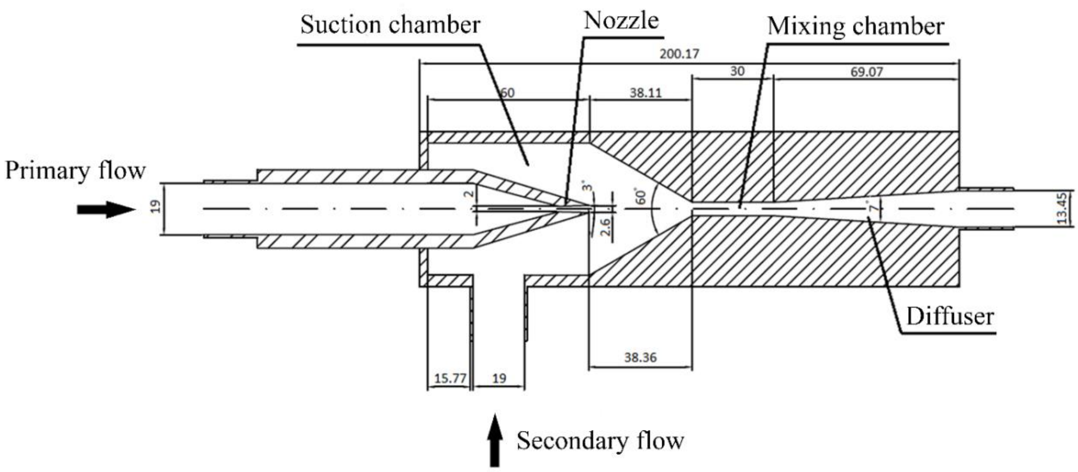

Figure 3. The ejector geometry [23]

Figure 4. Photograph of ejector

2.1. Thermodynamic Analysis of the Experimental System

The equations used to calculate the performance parameters are given in Table 1. The equations were created based on the pressure-enthalpy diagrams provided in Figure 5. Table 2 presents the results of the uncertainty analysis conducted for the performance parameters.

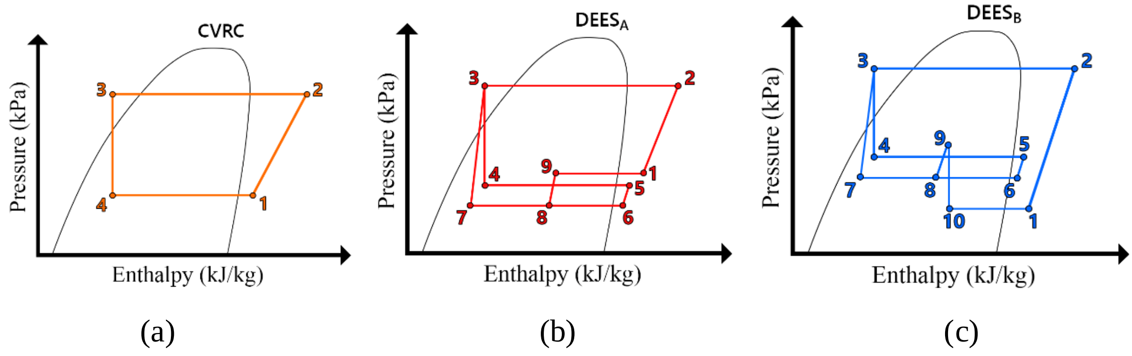

Figure 5. Pressure – entalpy diagrams a) CVRC b) DEES$_A$ c) DEES$_B$

Table 1. Thermodynamic equations

	CVCR	DEES$_A$	DEES$_B$
Evap#1 cooling capacity (kW)	$\dot{Q}_{(evap\#1)} = (h_5 - h_4)\dot{m}_1$	$\dot{Q}_{evap\#1} = (h_5 - h_4)\dot{m}_2$	$\dot{Q}_{evap\#1} = (h_5 - h_4)\dot{m}_2$
Evap#2 cooling capacity (kW)	–	$\dot{Q}_{evap\#2} = (h_9 - h_1)\dot{m}_1$	$\dot{Q}_{evap\#2} = (h_{10} - h_1)\dot{m}_1$
Total cooling capacity (kW)	$\dot{Q}_{evap,total} = \dot{Q}_{evap\#1}$	$\dot{Q}_{evap,total} = (\dot{Q}_{evap\#1} + \dot{Q}_{evap\#2})$	$\dot{Q}_{evap,total} = (\dot{Q}_{evap\#1} + \dot{Q}_{evap\#2})$
Compressor Work (kW)	$\dot{W}_{comp} = (h_2 - h_1)\dot{m}_1$	$\dot{W}_{comp} = (h_2 - h_1)\dot{m}_1$	$\dot{W}_{comp} = (h_2 - h_1)\dot{m}_1$
COP	$COP_{CVCR_A} = \frac{\dot{Q}_{evap\#1}}{\dot{W}_{comp}}$	$COP_{DEES_A} = \frac{\dot{Q}_{evap,total}}{\dot{W}_{comp}}$	$COP_{DEES_B} = \frac{\dot{Q}_{evap,total}}{\dot{W}_{comp}}$

Table 2. Presents the results of the uncertainty analysis conducted for the performance parameters

	CVCR	DEES$_A$ - DEES$_B$
Evaporator#1 (%)	0.41	0.41
Evaporator#2 (%)	-	0.68
Total cooling capacity (%)	0.40	0.92
W_{net} (%)	0.24	0.24
COP (%)	2.32	4.03

3. RESULTS AND DISCUSSION

In this section, the results of experiments performed in CVCR, $DEES_A$, and $DEES_B$ modes are analyzed. The system was operated for 30 minutes prior to the experiments. The inlet and outlet temperatures of the WHL water tank were recorded at one-minute intervals. Table 3 lists the active and inactive system components for each configuration.

Table 3. Active and inactive system components

	Cond	Evap#1	Evap#2	TXV#1	TXV#2	Ejector
CVRC	+	+	–	+	–	–
$DEES_A$	+	+	+	+	–	+
$DEES_B$	+	+	+	+	+	+

The variation of the performance parameters depending on the condensing temperatures (ct) is given between Fig. 6 and Fig. 9. Condenser temperatures are the temperatures corresponding to the pressures measured at the inlet of the condenser. When Fig. 6 is examined, it can be observed that the mass flow rates increase in all configurations as the ct increase. Furthermore, when the system is operated in $DEES_A$ mode, it is seen that the mass flow rates are higher than in other modes. For instance, at a compressor outlet pressure of 1050 kPa, the mass flow rates of the $DEES_A$ configuration are 81% higher than those of the $DEES_B$ configuration and 25% higher than those of the CVCR configuration. When the system operates in $DEES_A$ mode, the velocity of the refrigerant flowing from the primary inlet of the ejector increases despite the decrease in pressure in the nozzle section. Moreover, the density of the refrigerant at the diffuser outlet increased depending on the increase in pressure and temperature. Consequently, the mass flow rates increased with the increase in velocity and density.

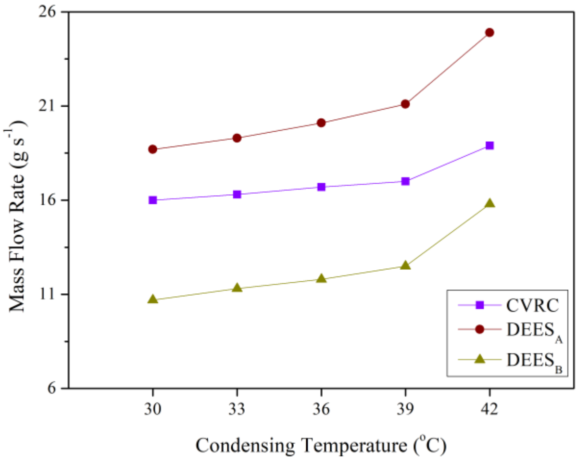

Figure 6. Variation of mass flow rate depending on condensing temperature

The changes in compressor inlet pressure values for three different configurations based on the ct values are given in Figure 7a. In all configurations, as the ct increased, the compressor inlet pressure values also increased. The highest compressor inlet pressure values were observed in the $DEES_A$ configuration. For a ct of 36 °C, the compressor inlet pressure in $DEES_A$ was 71% higher than $DEES_B$ and 24% higher than CVCR. The reason for the higher compressor inlet pressures in $DEES_A$ is that the ejector is utilized in this mode, and no throttling device is employed before evap#2. The compressor inlet pressure of the refrigerant increased when the ejector was active. Additionally, the effect of the throttling device used before evaporator#2 in reducing the compressor inlet pressure was greater than the effect of the ejector in increasing the compressor inlet pressure in $DEES_A$ mode, resulting in higher compressor inlet pressures compared to $DEES_B$. The changes in compressor power values for three different configurations based on the ct values are given in Figure 7b. As the ct increased, the compressor power values increased in all configurations. The highest compressor power was obtained when the system was operated in $DEES_A$ mode. At a ct 36 °C, the compressor power value in the $DEES_A$ configuration was 14% higher than $DEES_B$ and 11.5% higher than CVCR. The reason for this is the high mass flow rate and compressor inlet pressure values in $DEES_A$ mode.

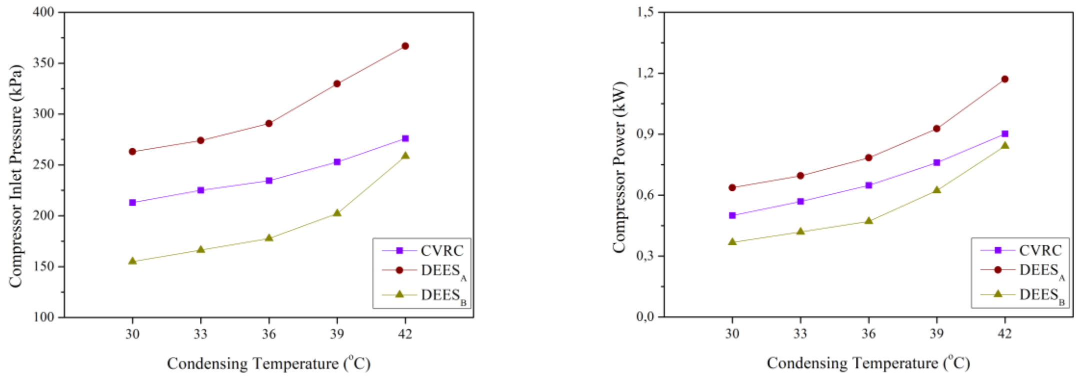

Figure 7. Variation of **a)** compressor inlet pressure **b)** compressor power depending on condensing temperature

The changes in the cooling capacity of evaporator#1 for three different configurations based on the ct are shown in Figure 8a. It can be seen that the cooling capacity of evaporator#1 increases for all configurations as the ct increase. When the system is operated as CVRC, evaporator#1 reaches its highest cooling capacity value. At a ct 36 °C, the evaporator#1 cooling capacity of the CVCR configuration was 60% higher than that of DEES$_A$. The reason for this is that in DEES$_A$ and DEES$_B$ modes, the refrigerant flow at the condenser outlet is split into two different paths, leading to a decrease in the amount of refrigerant flow passing through evaporator#1. However, in the CVRC mode, all refrigerant flow passes through evaporator#1. The reason why DEES$_A$ has a higher evaporator#1 cooling capacity than DEES$_B$ can be explained by the throttling device used before evaporator#2 reducing the flow rates. The changes in the total cooling capacity values of the three different configurations based on the ct are shown in Figure 8b. It can be seen that the total cooling capacity values for all configurations increase as the compressor discharge pressures increase. The total cooling capacity value is the sum of the cooling capacities of evaporator#1 and evaporator#2. The DEES$_A$ configuration has the highest total cooling capacity. For example, when the ct are 36 °C, the total cooling capacity of the DEES$_A$ configuration is 29% higher than that of DEES$_B$ and 33% higher than that of the CVRC configuration. It can be seen that DEES$_B$ has a lower total cooling capacity than CVRC, despite the use of an ejector. This is because the effect of the throttling device used before evaporator#2 to reduce the mass flow rate is greater than the effect of the ejector to increase the mass flow rate.

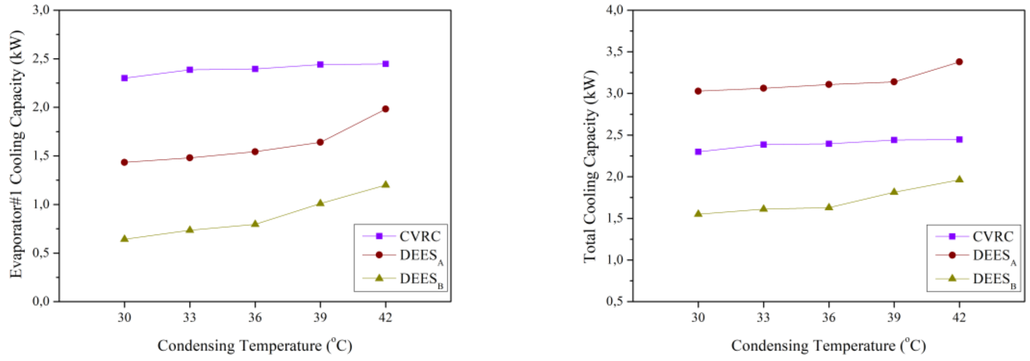

Figure 8. Variation of **a)** Evaporator#1 cooling capactiy **b)** Total cooling capacity depending on condensing temperature

The changes in COP of three different configurations depending on ct are given in Figure 8a. When examining Figure 9a, it can be seen that as the ct increase, the COP values decrease for all configurations. Despite its high compressor power, the configuration with the highest COP value is DEES$_A$. At a ct 36 °C kPa, the COP obtained from the DEES$_A$ configuration was respectively 14% higher than DEES$_B$ and 5% higher than CVRC. The reason for this is that the DEES$_A$ configuration has a high total cooling capacity. The changes in the subcooling degrees of three different configurations depending on the ct are given in Figure 9b. When examining Figure 8b, it can be seen that as the ct increase, the subcooling degrees increase for all configurations. The configuration with the highest subcooling degrees is DEES$_A$. The reason for this is the use of a second expansion valve before evaporator #2 in the DEES$_B$ mode. When Figure 9c is examined, it can be observed that the highest superheat degrees are obtained when the system operates in the DEES$_B$ configuration. This can be explained by the system operating at lower compressor inlet pressures in the DEES$_B$ configuration. Furthermore, it can be noted that as ct increase in the DEES$_B$ mode, superheat degrees decrease. The lowest superheat degrees are observed when the system is operated in the CVCR configuration. Compared to other configurations, superheat degrees were lower in the baseline system as it did not use a second evaporator and a TXV.

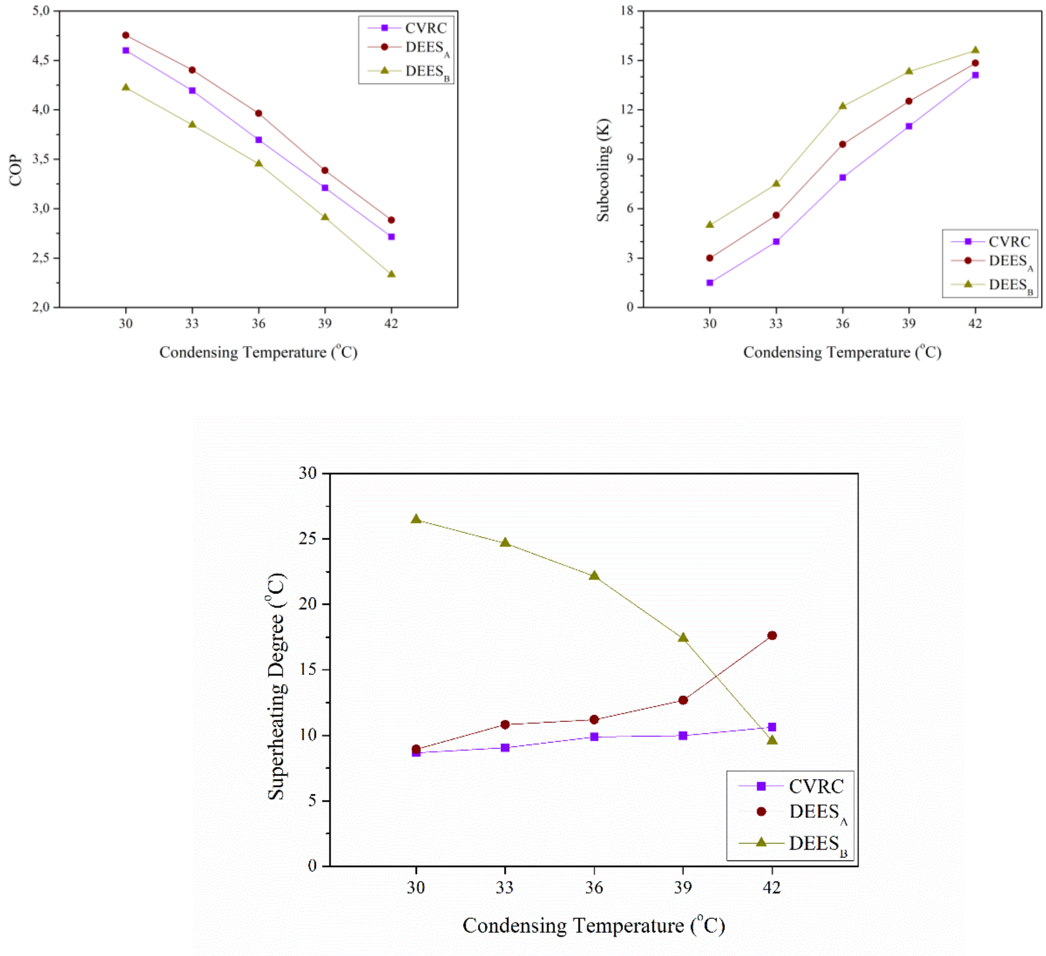

Figure 9. Variation of **a)** COP **b)** Subcooling and **c)** Superheat degrees depending on condensing temperature

All the results obtained from the comparison of DEES$_A$, DEES$_B$, and CVCR configurations are presented in Fig 10. When the system was operated in DEES$_A$ mode, higher total cooling capacity and COP were achieved compared to DEES$_B$ and CVCR. Figure 10 highlights the advantages of different configurations in the ejector-based refrigeration system when compared to each other. For instance, DEES$_B$ is considered superior when evaluating low evaporator temperatures, while DEES$_A$ outperforms in terms of energy consumption. According to Figure 10, it is also evident that the CVCR configuration exhibits lower performance than the configurations utilizing ejectors, except for the cooling capacity of evaporator#1.

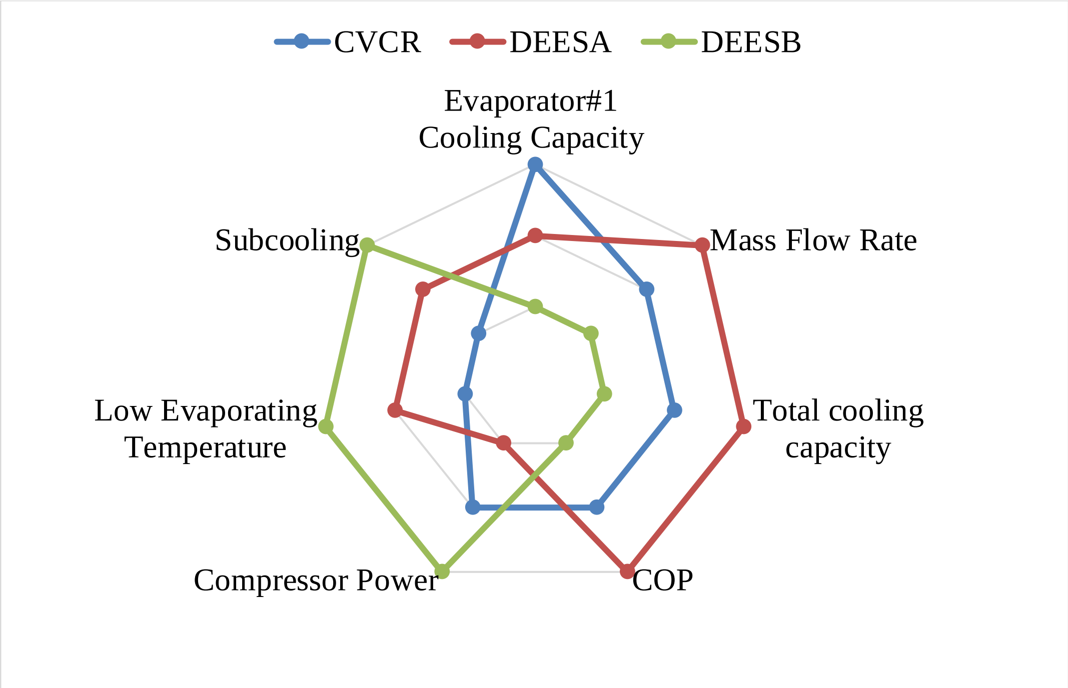

Figure 10. Comparison of $DEES_A$, $DEES_B$, and CVCR configurations

4. CONCLUSIONS

The aim of this study was to investigate the impact of an ejector on a refrigeration system. To achieve this objective, an experimental ejector refrigeration system was tested in different configurations under various condensing temperatures. The results indicate that the $DEES_A$ configuration achieved COP values up to 21% higher. Conversely, the $DEES_B$ configuration resulted in lower evaporation temperatures when compared to $DEES_A$. $DEES_B$ is considered superior when evaluating low evaporator temperatures, while $DEES_A$ outperforms in terms of total cooling capacity and COP. On the other hand, compared to other configurations, the superheat degrees were lower in the CVRC as it did not use a second evaporator. Furthermore, when the system is operated as CVRC, evaporator#1 cooling capacity is the highest. Finally, it was revealed that the ejector operates more efficiently in systems with dual evaporators, thereby making positive contributions to the overall system performance.

ACKNOWLEDGMENT

We are grateful to Yalova University due to financial support (Project No. 2021/YL/ 0020 and 2019/AP/0013).

DECLARATION OF ETHICAL STANDARDS

The authors of the paper submitted declare that nothing which is necessary for achieving the paper requires ethical committee and/or legal-special permissions.

CONTRIBUTION OF THE AUTHORS

Batuhan Üğüdür: Experimental investigations staff, Formal analysis, Writing - Original Draft,
Ümit İşkan: Experimental investigations staff, Writing - Original Draft
Mehmet Direk: Methodology, Conceptualization, Experimental investigations leadership, Writing - Original Draft, Writing - Review & Editing, Supervision

CONFLICT OF INTEREST

There is no conflict of interest in this study.

REFERENCES

[1] L. DJ. The Role of Refrigeration in the Global Economy (2019), 38th Note on Refrigeration Technologies. International Institute of Refrigeration, France, Paris, 2019.

[2] Direk M, Soylu E. The effect of internal heat exchanger using R1234ze(E) as an alternative refrigerant in a mobile air-conditioning system. Journal of Mechanical Engineering 2018;64:114-120.

[3] Erdinc MT. Two-evaporator refrigeration system integrated with expander-compressor booster. International Journal of Refrigeration 2023; 0140-7007.

[4] Erdinc MT. Performance simulation of expander-compressor boosted subcooling refrigeration system. International Journal of Refrigeration 2023;149:237-247.

[5] Prabakaran R, Lal DM, Kim SC. A state of art review on future low global warming potential refrigerants and performance augmentation methods for vapour compression based mobile air conditioning system. Journal of Thermal Analysis and Calorimetry 2023;148:417-449.

[6] Caliskan O, Ersoy HK. Energy analysis and performance comparison of transcritical CO_2 supermarket refrigeration cycles. The Journal of Supercritical Fluids 2022;189:105698.

[7] Oshitani H, Yamanaka Y, et al. Vapor Compression Cycle Having Ejector. United States Patent 2007; Patent No. US007254961B2.

[8] Lawrence N, Elbel S. Experimental investigation of a two-phase ejector cycle suitable for use with low-pressure refrigerants R134a and R1234yf. International Journal of Refrigeration 2014;38:310-322.

[9] Kim S, Jeon Y, Chung HJ, Kim Y. Performance optimization of an R410A air-conditioner with a dual evaporator ejector cycle based on cooling seasonal performance factor. Applied Thermal Engineering 2018;131:988-997.

[10] Bilir Sag N, Ersoy HK, Hepbasli A, Halkaci HS. Energetic and exergetic comparison of basic and ejector expander refrigeration systems operating under the same external conditions and cooling capacities. Energy Conversion and Management 2015;90:184-194.

[11] Ünal Ş, Yilmaz T. Thermodynamic analysis of the two-phase ejector air-conditioning system for buses. Applied Thermal Engineering 2015;79:108–116.

[12] Wang X, Yu J, Xing M. Performance analysis of a new ejector enhanced vapor injection heat pump cycle. Energy Conversion and Management 2015;100:242-248.

[13] Geng L, Liu H, Wei X, Hou Z, Wang Z. Energy and exergy analyses of a bi-evaporator compression/ejection refrigeration cycle. Energy Convers Manag 2016;130:71-80.

[14] Expósito Carrillo JA, Sánchez de La Flor FJ, Salmerón Lissén JM. Thermodynamic comparison of ejector cooling cycles. Ejector characterisation by means of entrainment ratio and compression efficiency. International Journal of Refrigeration 2017;74:371-384.

[15] Gao Y, He G, Cai D, Fan M. Performance evaluation of a modified R290 dual-evaporator refrigeration cycle using two-phase ejector as expansion device. Energy 2020;212.

[16] Liu J, Liu Y, Yu J. Performance analysis of a modified dual-ejector and dual-evaporator transcritical CO_2 refrigeration cycle for supermarket application. International Journal of Refrigeration 2021;131:109–118.

[17] Direk M, İşkan Ü, Tunçkal C, Mert MS, Yüksel F. An experimental investigation of ejector employed a dual-evaporator vapor compression refrigeration system under various entrainment ratios using R134a as the refrigerant. Sustainable Energy Technologies and Assessments 2022;52:102293.

[18] Alkhulaifi YM, Qasem NAA, Zubair SM. Exergoeconomic assessment of the ejector-based battery thermal management system for electric and hybrid-electric vehicles. Energy 2022;245:123252.

[19] Ünal Ş, Erdinç MT, Akgün H, Bilgili M. Effects of alternative refrigerants on the ejector dimensions for single and dual ejectors enhanced bus air conditioning system. International Communications in Heat and Mass Transfer 2023;143:106685.

[20] Direk M, İşkan Ü, Üğüdür B, Kahraman MC. Experimental performance analysis of ejector heat pump water heater under transient conditions. Sci Technol Built Environ 2023;29:523-532.

[21] Tahir Erdinc M, Kutlu C, Unal S, Aydin O, Su Y, Riffat S. Performance improvement potential of a PV/T integrated dual-source heat pump unit with a pressure booster ejector. Thermal Science and Engineering Progress 2023;37:101534.

[22] İşkan Ü, Direk M. Experimental performance evaluation of the dual-evaporator ejector refrigeration system using environmentally friendly refrigerants of R1234ze(E), ND, R515a, R456a, and R516a as a replacement for R134a. J Clean Prod 2022;352:131612.

[23] İşkan Ü, Üğüdür B, Kahraman MC, Direk M, Tunçkal C. Evaluation of the impact of the temperature and mass flow rate of the water, utilized in the R516A refrigeration system with dual evaporator and ejector, on the performance parameters. Energy Sources, Part A: Recovery, Utilization, and Environmental Effects 2022; 44:7316-7329.